2019

# SNS OPTICAL FIBER STRUCTURE SENSOR FOR DIRECT DETECTION OF THE PHASE TRANSITION IN C18H38 N-ALKANE MATERIAL

Wei Han
*Technological University Dublin*

Marek Rebow
*Technological University Dublin*, marek.rebow@tudublin.ie

Xiaokang Lian
*PRC*, d15128010@mydit.ie

*See next page for additional authors*



## Recommended Citation

Han, W., Rebow, M., Lian, X., Liu, D., Farrell, G., Wu, Q., & Semenova, Y. (2019). SNS optical fiber sensor for direct detection of phase transitions in C18H38 n-alkane material. *Experimental Thermal and Fluid Science,* 109854. DOI:10.1016/j.expthermflusci.2019.1098...

# SNS OPTICAL FIBER STRUCTURE SENSOR FOR DIRECT DETECTION OF THE PHASE TRANSITION IN C18H38 N-ALKANE MATERIAL

*Wei Han[1], Marek Rebow[2], Xiaokang Lian[1], Dejun Liu[1], Gerald Farrell[1], Qiang Wu[3], Youqiao Ma[4] and Yuliya Semenova[1]*

[1]Photonics Research Centre, Technological University Dublin, Kevin Street, Dublin 8, Ireland

[2]College of Engineering and Built Environment, Technological University Dublin, Bolton Street, Dublin 1, Ireland

[3]Department of Mathematics, Physics and Electrical Engineering, Northumbria University, Newcastle Upon Tyne, NE1 8ST, United Kingdom

[4]Depatment of Electrical and Computer Engineering, Dalhousie University, Halifax B3H 4R2, Canada

Key words: Optical fiber sensor, Phase change materials (PCMs), n-octadecane, Supercooling

## Abstract

A singlemode-no-core-singlemode (SNS) fiber structure optical sensor for detecting the solid-liquid phase change in a phase change material: C18H38 n-alkane material (n-octadecane) is proposed and demonstrated. The transmission-type sensor probe consists of a short section of no-core fiber sandwiched between two sections of a singlemode fiber. Phase changes in n-octadecane are accompanied by large step-like variations of its refractive index (RI). Such a large discontinuous change of the n-octadecane's RI during its phase transition, leads to the corresponding step-like change in the transmitted optical power that can reliably indicate the phase change of the sample in the vicinity of the sensor. In addition, the proposed sensor can detect whether the sample is in solid or liquid phase based on a single power measurement, can detect supercooling, and is resistant to bending and strain disturbances during the measurements. The results of this work also illustrate that the proposed sensor can be applied to detect liquid-solid phase changes in other materials with thermo-optic properties similar to n-octadecane.

## Introduction

Phase change materials (PCMs) are widely used in thermal energy storage applications due to their ability to absorb, store and release large amounts of energy during melting or solidification. To achieve higher efficiency in energy storage applications, it is necessary to be able to accurately detect the phase changes in PCMs. A typical indirect approach for detection of phase changes in a PCM involves monitoring of the material temperature with standard electrical sensors, such as thermocouples. However this approach has some limitations. For example, due to its high thermal conductivity, a thermocouple can act as a local source of heat immersed within a sample, which in turn may affect the phase state in its vicinity and thus cause errors in the phase change detection [1]. Moreover, where supercooling occurs (a phenomenon during which the PCM remains in liquid phase even if its temperature is lower than the solidification point), the measurement of the temperature alone does not provide reliable information regarding the phase state of the PCM.

Therefore in practice, direct detection of the phase changes in PCM is preferred. For optically transparent materials, direct observation of the solid-liquid interface is possible [2]. However

this method is not suitable for opaque materials. Since the different phases of the material have different ability of X-ray absorption, X-ray imaging allows the visualization of solid-liquid interfaces regardless of optical transparency [3] so the method can detect changes in the material density associated with the phase changes, but it is laboratory-based and involves high cost, besides this method potentially involves exposure of human personnel to radiation. During melting or cooling, most PCMs show changes in electrical resistance, thus resistance diagnostics has also been used for the detection of phase change [4]. It is a safe and low cost technology compared to the X-ray method, but again it has the disadvantage of complexity. Differential scanning calorimetry (DSC) can be applied to characterize PCMs, and it also can be used to detect the phase state within a very small bulk material sample [5]. However, it is not capable of detecting the phase state at a specific point within the sample's volume, and thus it is not suitable for energy storage applications which involve large PCM volumes.

Fiber optic sensors offer the advantages of a simple structure, high sensitivity, low cost, and immunity to electromagnetic interference making them popular candidates for measurements of many physical parameters, including temperature [6-7] and strain [8-9]. Several studies considered applications of fiber optic sensors in detection of phase changes. For example, Arnon *et al.* [10] developed a fiber-optic evanescent wave spectroscopic method for detecting the solid-liquid phase changes in water based on the changes of the sample's absorbance. However the technique is relatively complex and requires the use of special silver halide based fibers. Mani *et al.* [11] reported a Fresnel reflection fiber sensor for monitoring the crystallization of water and aqueous solution of NaCl by detecting the changes of the reflected power ratio from the probe. Recently Wei et al. investigated the use of a similar Fresnel reflection fiber probe for detecting phase changes in n-octadecane [12]. Although this method is simple and accurate, it requires multiple measurements to realize continuous optical power monitoring since it relates the phase change to a relative change in the reflected optical power by the probe. Moreover, such Fresnel sensors are highly susceptible to disturbances within the material, including fluctuations in reflections due to bubbles or impurities, making it less reliable in real world applications.

In this paper we propose and experimentally demonstrate a novel fiber optic sensor for in-situ detection of the solid-liquid and liquid-solid phase changes in n-octadecane. The sensor probe is fabricated by splicing a section of no-core fiber between two sections of a standard single-mode fiber (SMF). The phase change is detected by monitoring the output normalized power change transmitted by the sensor probe immersed into the sample. C18H38 n-alkane material is a popular PCM (n-octadecane), whose thermal characteristics make it attractive for a number of applications, including thermal control in a spacecraft [13], or in comfort clothing, to maintain the appropriate temperature close to that of human skin [14]. In this work n-octadecane was chosen for the proof of principle demonstration of the proposed sensing method because the material's crystallization occurs over a narrow range of temperatures, with a high degree of repeatability. In addition, the closeness of the solidification point to room temperature allows for a simpler experimental set up. Moreover, the material is transparent in the liquid phase and opaque in the solid phase, which makes it possible to observe the phase change in the vicinity of the probe as the means of validation of the proposed sensor. Besides, a lot of alkane materials have similar characteristics to n-octadecane, so that the detection for the phase change of the n-octadecane can be used to validate the numerical models of melting and solidification for other alkane materials and their applications [15].

The method proposed in this work allows for a simple, low cost, accurate and reliable in-situ detection of liquid-solid and solid-liquid phase changes in n-octadecane without the need for temperature measurements. Compared to our previous study [12], this method has the

significant advantage that it allows detection of the specific phase state based on a single measurement. Moreover, after transforming the analogue output into a digital signal, the small disturbances of the output power due to the presence air bubbles, voids and impurities can be eliminated, which makes the proposed sensor resistant to disturbances in practical applications.

## Experimental setup and operating principle

The proposed sensor system is shown in Figure 1. To eliminate the effect of fluctuations in the light source power output over time, a ratiometric scheme has been used that determines the ratio between the output power from the sensor and that from a reference arm [12]. The system consists of a 3 dB coupler, the input port of which is connected to a laser (1560, NETTEST, wavelength: 1550 nm), one of the outputs of the coupler is connected to one of the channels of an optical power meter (4100, Dbm Optics) as a reference and another output is connected to the fiber sensor and an optical power meter in a sequence. The sensor probe to be immersed into a sample of n-octadecane is fabricated from a short section of no-core fiber spliced between two sections of standard single-mode fiber. The coating is stripped from the no-core fiber section and the single-mode fiber near the no-core section is marked with blue ink to allow better observation of the probe's position when it is immersed. In addition since the liquid phase sample is transparent while the solid phase sample is not, visual observation of the blue mark can indicate a point where the sample is in liquid phase. The temperature in the vicinity of the fiber sensor probe was monitored with a K-type thermocouple which is fixed near the probe, to detect the temperature of the sample at the location where the probe is. The thermocouple has an error of $\pm 0.004 \times T$, where $T$ is the actual temperature. A Peltier element is used as a thermoelectric heater/cooler.

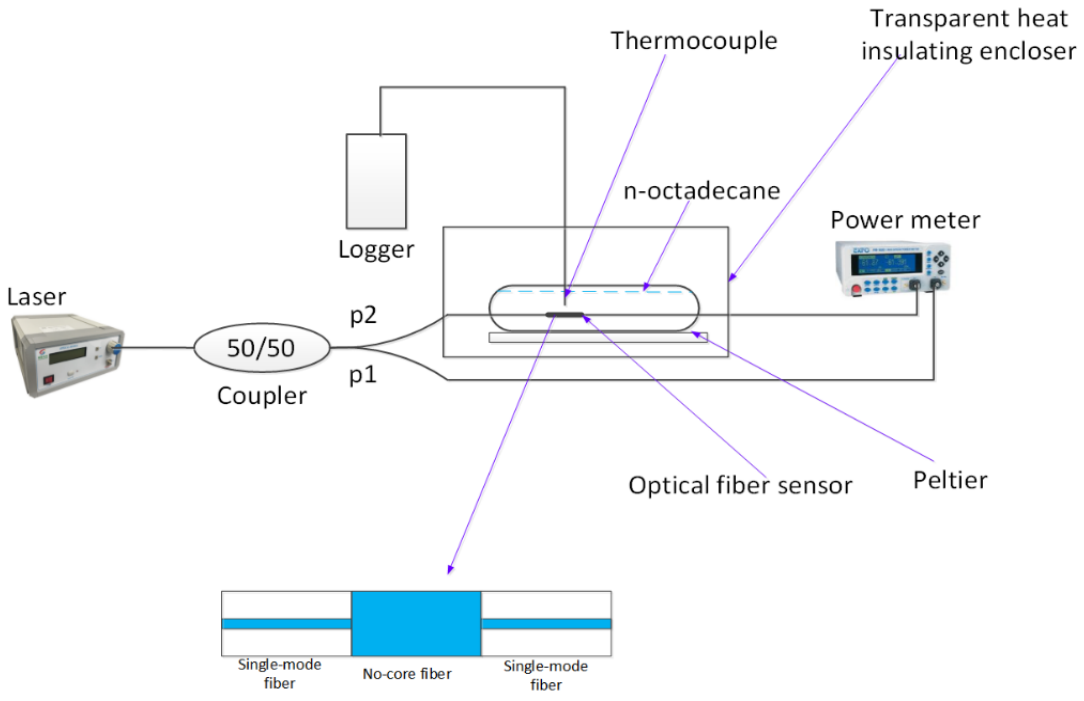


Fig. 1. Schematic diagram of the experimental setup.

Assuming the input and output single-mode fibers are the same and the length of no-core fibre is L, when the sensor is immersed in the solid sample, whose RI is higher than that of

the no-core fiber, the field in the no-core fiber consists of leaky modes and the output of the sensor can be described as [16]:

$$\mathrm{P} = 10log_{10}\left(\frac{|\int_0^\infty E(L)E_0 ds|^2}{\int_0^\infty |E(L)|^2 ds \int_0^\infty |E_0|^2 ds}\right) \quad (1)$$

where *E(L)* is the electrical field at the end of no-core fiber, $E_0$ is the electrical field of the fundamental mode of the single-mode fiber. The electrical field of the leaky mode in the no-core fiber can be described as [16]

$$E(L) = \sum_{m=1}^{M} b_m E_m e^{i\beta_m L} e^{-a_m L} \quad (2)$$

where $E_m$ and $b_m$ are electrical field and excitation coefficients of the m$^{th}$ leaky mode in the no-core fiber respectively, $\beta_m$ and $a_m$ are the propagation constant and attenuation constants respectively and *M* is the total number of modes in the no-core fiber.

When the sensor is immersed in the liquid sample whose RI is lower than that of the no-core fiber, the field of the no-core fiber consists of guided modes which can be described as [17]

$$E(L) = \sum_{m=1}^{M} b'_m E'_m e^{j\beta'_m L} \quad (3)$$

where $b'_m$ is the excitation coefficient of each mode, $E'_m$ are the eigenmodes of the no-core fiber and $\beta'_m$ are the propagation constants of each eigenmode of the no-core fiber.

From [18], the RI values for n-octadecane are known to be approximately 1.468 for the solid and 1.432 of liquid phases at a wavelength of 600 nm. We have used the data in [18] and the Cauchy's equation [19] to calculate the approximate values of the refractive index of the n-octadecane in the wavelength range of interest for our experiment. The results of the calculations showed that the RI of n-octadecane at a wavelength of 1550 nm decreases by only by 0.08% for the solid and by 0.07% for the liquid phase, by comparison to the values at 600 nm. The RI of n-octadecane decreases with temperature: while in its solid phase it experiences only a small decrease with the increase in temperature, but as soon as the n-octadecane becomes liquid, its RI decreases sharply from circa 1.468 to 1.432 [18]. The RI of the no-core fiber is 1.444. When the sensor is immersed in the solid n-octadecane, since the RI of the material sample is higher than that of the no-core fiber, light propagating through the no-core section is no longer confined to the fiber due to the absence of total reflection, which results in low power output from the sensor. As soon as the n-octadecane melts into liquid, the RI of the sample decreases toapproximately 1.432, becoming lower than the RI of the no-core fiber. The modes with the incident angle larger than the critical angle will be totally reflected so the output power increases sharply. Therefore the phase state of the n-octadecane sample can be detected by measurement of the transmitted power (low or high), and the phase change can thus be determined by detecting the step-like change in the sensor's output.

Figure 2 illustrates the simulated optical power distribution within the no-core fiber section and the transmitted output powers for the sensor immersed in the n-octadecane before and after melting. The Z axis is the direction of the light propagation, and the X axis is the transverse direction which is vertical to the direction of the light propagation. The monitor value shows the intensity of the light on the Z axis. The simulations have been carried out using commercial software package BeamPROP (Rsoft, Pasadena, CA, USA). In the simulations the free space wavelength was set as 1550 nm, the RI of the single-mode fiber core and cladding were set as 1.468 and 1.44 respectively, and the RI of the no-core fiber was set as 1.444. The lengths of the two sections of the single-mode fiber spliced with the no-core fiber were set as 1 mm and

the length of the no-core fiber was set as 5 mm, which is the same as the length of the sensor using in the experiment. The reason for choosing such a short length is to ensure an acceptable measurement spatial resolution. The diameters of the core and the cladding of the single-mode fiber are taken as 8.3 µm and 125 µm, the diameter of the no-core fiber was set as 125 µm. In the simulations the RI of the solid n-octadecane was assumed equal to 1.468 and the liquid n-octadecane RI was set as 1.432. From the simulation it can be seen, that when the material sample is solid (Fig. 2a), the light power launched from the first single-mode fiber section into the no-core fiber (Z=100 µm) leaks out of the no-core fiber into the solid sample whose RI is higher than that of the no-core fiber, causing the low power output of the sensor. As soon as the sample melts into a liquid (Fig. 2b), the RI of the material sample becomes smaller than that of the no core fiber, so that the light power is more strongly confined within the no-core fiber section leading to a higher power coupled back into the second single-mode fiber and thus to the higher output of the sensor.

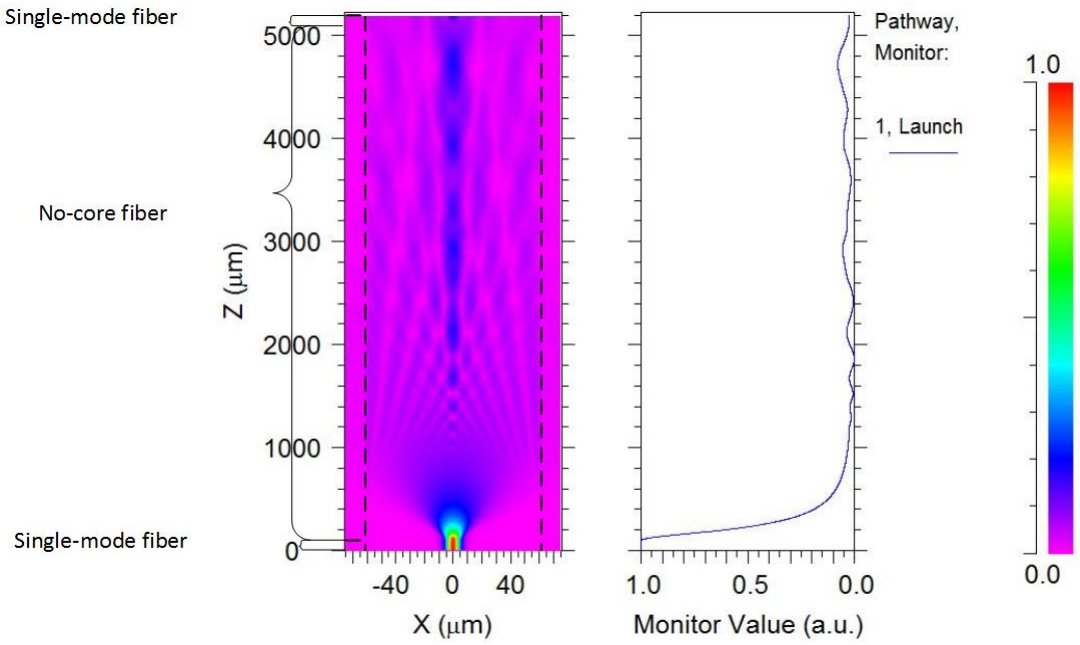


a

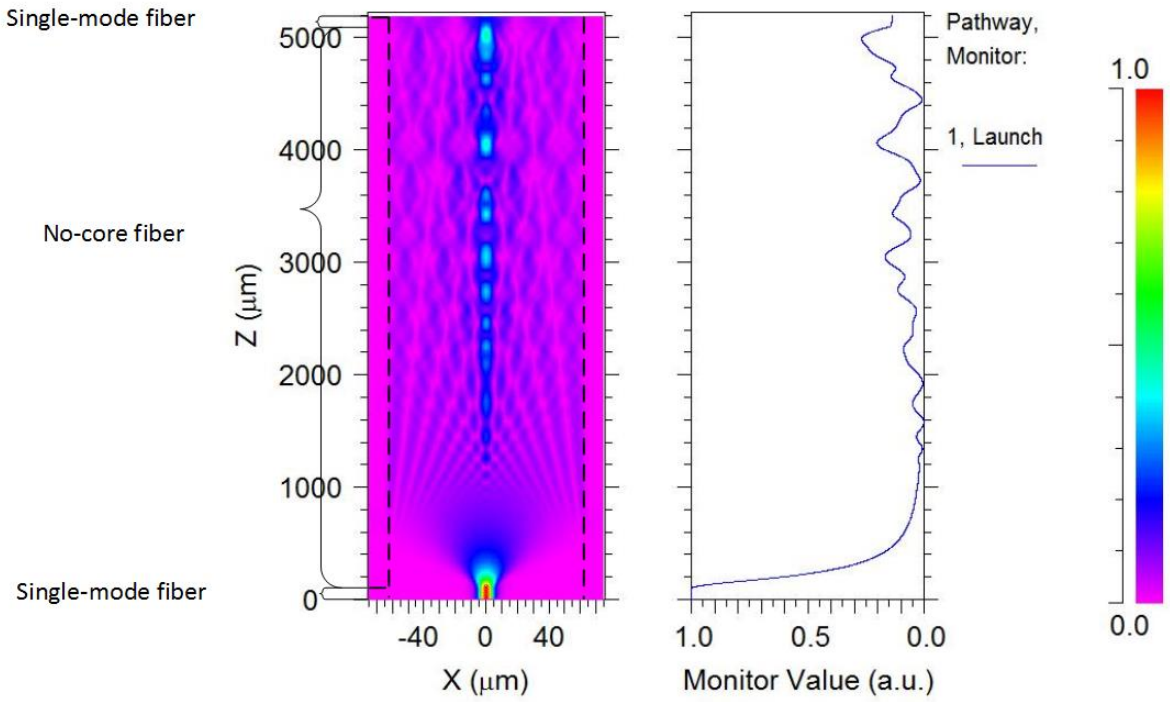


b

Fig.2 Simulated output power distributions (left) and intensity of the light on the Z axis (right) when the sensor is immersed in: (a) solid, (b) liquid sample.

## Experimental results and discussion

Before using the sensor for phase change detection, the sensor is initially characterized in air prior to immersion in the PCM. The sensor is connected with a broadband optical source and the optical spectrum analyzer is used to measure the spectral response as shown in Fig. 3. From the figure it can be seen that the output power varies as wavelength changes, but the difference is less than 4.5 dB over a wide wavelength range from 1520 nm to 1600 nm. In our experiments the laser wavelength was set at 1550 nm as an optical source for the phase change measurement experiments.

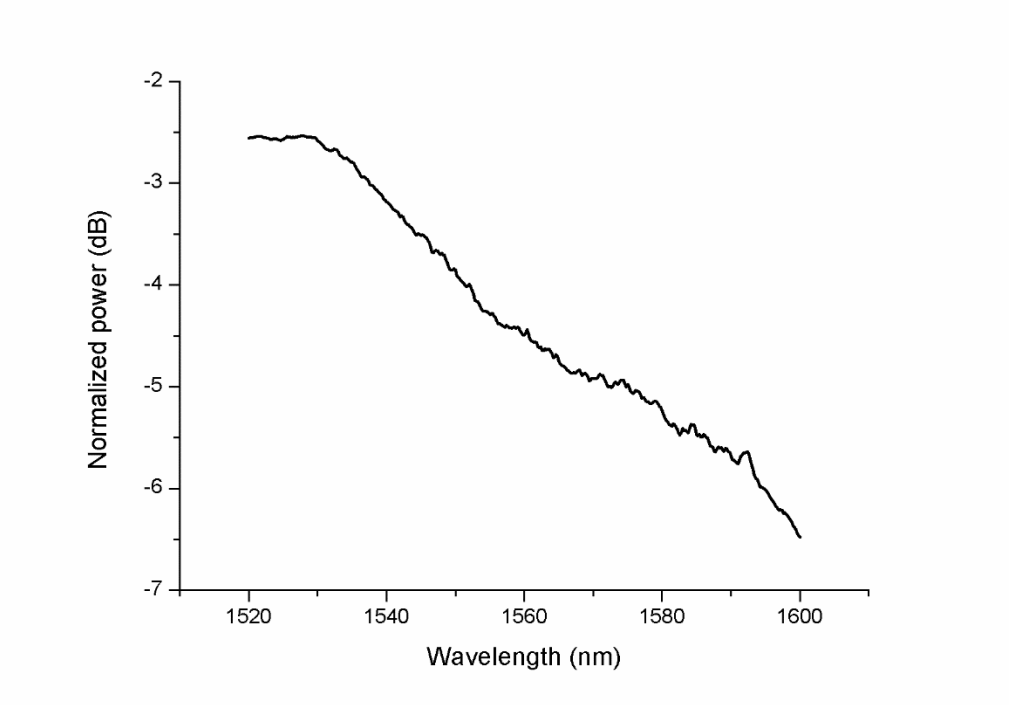


Fig.3 the spectrum of the sensor

In order to experimentally demonstrate the operation of the proposed sensor, a series of heating and cooling experiments were carried out for a 25 ml sample of n-octadecane with 99% purity (Sigma Aldrich), using the experimental setup shown in Figure 1. The fiber probe and the thermocouple are immersed into the n-ocatdecane sample with the distance between the fiber probe and the thermocouple set at approximately 2 mm. The thermocouple was connected to a logger to record the temperature of the n-octadecane close to the fiber sensor probe. A digital camera was also placed inside the enclosure and connected with a laptop for recording images. The camera shutter was controlled by a PC. The photo images were taken at the same time as the reflected power and temperature data were recorded with steps of 0.5 °C.

For the heating case the Peltier heater was set so that the hot side of the heater was at a temperature of 50 °C and thus pumped heat into the sample, causing progressive melting of the sample that propagated slowly up through the sample, so that a visible interface between the solid and liquid phases could be seen moving up through the sample and could be visibly recorded by the camera.

For the cooling case the Peltier heater current direction was reversed so that the cold side of the heater touched the sample, whose temperature was set as 20 °C, causing solidification of the sample that propagated slowly up through the sample and again produced a visible interface between the liquid and solid phases that could be again visibly recorded by the camera.

To ensure the stability of the surrounding temperature, the experimental setup was placed inside a transparent heat insulating enclosure. For the heating case the temperature of the environment surrounding the sample was set to 20 °C, well below the temperature range of interest near the phase change point (circa 27.5 °C). This was done to ensure that the temperature of the surrounding environment did not inadvertently cause sporadic phase changes in the sample thus the only heat source that could cause a phase change was the heater. In turn this resulted in a well-defined interface between the solid and liquid n-octadecane that

was easily and repeatably observable by the camera. For the cooling case to ensure a well-defined sharp interface between the solid and liquid n-octadecane, the temperature of the surrounding environment was set to 30 °C, so that as for the heating case the local environment did not inadvertently cause sporadic phase changes in the sample.

Based on data returned by the sensor and the thermocouple, Figure 4 illustrates the dependence of the normalized output power of the sensor probe versus the temperature of n-octadecane during its heating cycle.

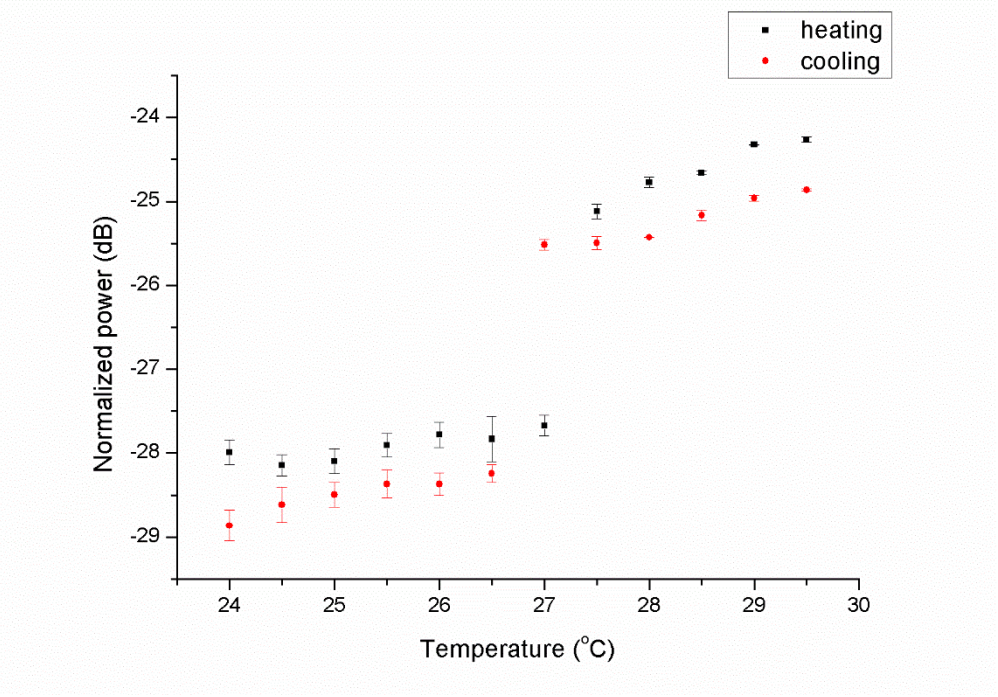


Fig.4 The response curve of the experiments

Every data point of the heating experimental result in Fig. 4 is an average of five different heating experiments. The average error of the data when the sensor is in the solid sample is 0.158 dB, the average error of the data when the sensor is in the liquid sample is 0.042 dB. One possible reason for the difference in errors for the two phases is the stronger influence of strain and stress acting upon the sensor in the solid state in comparison with those in the liquid state.

As can be seen from Fig. 4, in the range of temperatures from 24 °C to 27 °C the normalized transmitted power experiences minor fluctuations ranging from -27.99 dB to -27.67 dB. Since the RI of the solid n-octadecane is approximately 1.47, which is higher than the RI of the no-core fiber, the output power is low. As soon as the temperature of the n-octadecane reaches 27.5 ºC the sample melts into a liquid and its RI decreases to approximately 1.42, which is lower than the RI of the no-core fiber. Thus the light rays with an incident angle larger than the critical angle experience total internal reflection, which causes a sudden increase in the transmitted power. The critical angle can be described as [15]

$$\theta_c = arcsin\frac{n_2}{n_1} \tag{5}$$

As the temperature increases further, the RI of the n-octadecane decreases, leading to the decrease of the critical angle. This means that greater proportion of the optical power is

confined to the no-core fiber, causing a slight increase in the output power with temperature of the liquid.

The recorded images show that the sensor output step change aligns very well with the visible change recorded. Figure 5 shows images of the n-octadecane sample taken at different temperatures during the heating experiment. From the photos it can be seen that at 27 °C the sensor is not visible, which means the sample surrounding the sensor is solid, while at 27.5 °C the fiber sensor is visible, which proves that above 27.5 °C the sample surrounding the sensor is in the liquid phase.

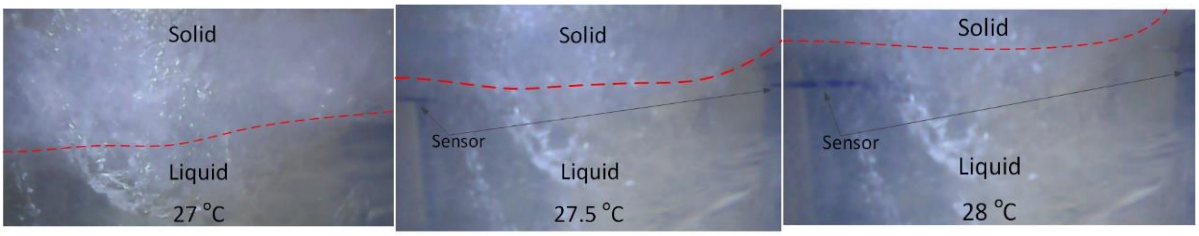


Fig.5 Photographs of the sample at different temperatures during heating experiment

Figure 4 also illustrates the dependence of the measured normalized output power of the sensor probe versus the temperature of n-octadecane during its cooling cycle.

Every data point of the cooling experiment in Fig. 4 is an average of five different cooling experiments. The average error of the data when the sensor is in the solid phase is 0.155 dB, the average error of the data when the sensor is immersed in liquid is 0.043 dB. As previously, the average error is higher when the sensor is inside the solid sample.

As the liquid sample is cooled from 29.5 °C to 27 °C, the probe's output power decreases slightly from -24.86 dB to -25.52 dB, which is consistent with a temperature-induced increase of the material's RI in the liquid phase. When the temperature decreases to 26.5 °C the n-octadecane sample solidifies. The output power decreases immediately from -25.52 dB to -28.24 dB as there is no total reflection for light rays in the no-core fiber section. Fig. 6 illustrates images of the n-octadecane sample taken at different temperatures during the cooling. From the photos it can be seen that at 27.5 °C and 27 °C the sensor is visible, which means the sample surrounding the sensor is liquid, while at 26.5 °C the fiber sensor is no longer visible, which proves that from 26.5 °C the sample phase surrounding the sensor is solid.

The phase change temperature in the cooling experiment is lower than the one in the heating experiment due to the hysteresis, which is the phenomenon that the solidification temperature of the sample is lower than the melting temperature. Moreover, there is a difference in the normalized power in the heating and cooling experiment. The most probable reasons for this are that the interface between liquid and solid may not be completely horizontal and straight, so that as the interface moves up or down through the sample the temperature surrounding the sensor may be slight different from the one surrounding the thermocouple and that the difference of the temperature between the sample for these two positions is not the same for the heating and the cooling cases, which also causes an error. Another reason for the difference is the variation in the force direction and value applied on the fiber caused by the slight volume change of the sample as it moves from one phase to another. In the cooling case the volume

decrease of the sample applies force to the sensor but in the heating case the volume increases for the sample which releases force.

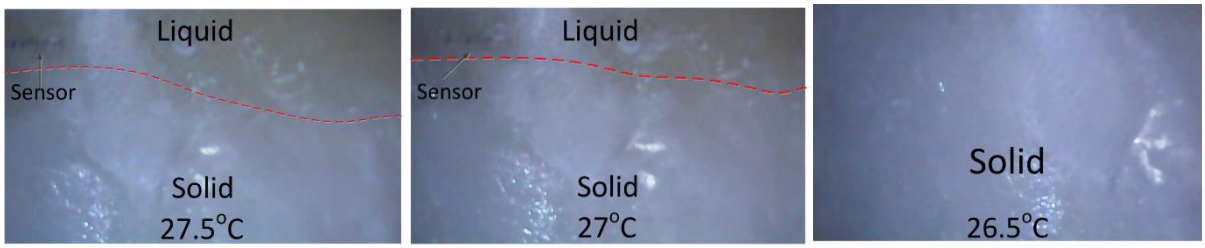


Fig.6 Photographs of the phase change front at different temperatures during cooling.

From the above experiments it can be seen that due to the sudden change of the RI of the sample associated with solid-liquid or liquid-solid phase transitions, the output power level from the sensor probe can be used as a measure or an indicator of the material's phase: the output power is low when the sensor is immersed into a solid n-octadecane and if the sensor is immersed into a liquid n-octadecane, the output power is high. Therefore the specific phase can be detected by a single measurement, which is an improvement compared to the sensor we proposed previously, since that sensor needs at least two distinct measurements to detect the phase of the sample [12].

Signal processing can be used to improve the reliability of detection of the phase change. The first step in signal processing is to digitize the outputs from the sensor fiber and the reference fiber following optoelectronic conversion. Subsequently software based averaging and noise reduction using low pass filtering or more sophisticated signal processing can be carried out to improve the signal-to-noise ratio. Finally the sensor output power level is compared to a reference power level with the reference optical power level chosen as an intermediate power output equidistant from the lowest and highest possible outputs from the sensor, recorded during the heating/cooling cycles. The result from the comparison will indicate either solid or liquid phases. The input from the reference fiber can be used to fine tune the reference level used, so as to eliminate the effect of optical source power variations. In addition if the proposed sensor is used together with a thermocouple, identification of a supercooled state should be possible, in which case the thermocouple would indicate a low (below solidification point) temperature while the output of the fiber optic sensor would remain high.

To study of the sensor's ability to operate in non-laboratory conditions where temperature and thermal convection changes are less controlled and less predictable, another cooling experiment was carried out, during which the temperature inside the enclosure was set to 15 °C and liquid n-octadecane was left to cool naturally. The initial temperature of the n-octadecane was 30 °C. Unlike cooling from the bottom of the container in the former experiment, in this case cooling of the sample occurs from its outer walls towards the center of the sample, so that the increasing pressure (due to the increasing sample density) is applied to the fiber from all directions. In such conditions there is no visible solid-liquid interface and the phase change is likely to be affected by various random factors. This in turn may result in larger fluctuations of the sensor output. The purpose of this experiment was to evaluate the performance of the sensor in such conditions, and its results are illustrated in Figure 7, where each point is an average of five measurements. As it can be seen from the figure, in the temperature range from 24 °C to 26.5 °C, the power changes from -28.84 dB to -28.47 dB, which means that the sensor's output

is low and the n-octadecane is in its solid state in the vicinity of the sensor. In the temperature range from 27 °C to 29 °C the output power changes from -25.22 dB to -24.56 dB. The output power is high indicating that the sensor is immersed in liquid n-octadecane.

Every data point in Fig. 7 is an average of five different cooling experiments. The average error of the whole experiment result is 0.16 dB. Compared to the previous experiment (Fig.4), the average error is larger and there is even a small decrease in the power output when the sample is in the liquid phase, which did not occur previously (Fig.4). One possible explanation is that in the latter experiment, the changes in the values and direction of the bending and strain applied to the fiber immersed in the sample were random during the whole process. However, even though the bending and the strain change randomly, it can be seen from Fig.8 that the information provided by the sensor allows for the unambiguous detection of the occurrence of solidification at 26.5 °C, which is exactly the same result as in the former experiment. It is can be concluded thus that the sensor is capable of providing reliable phase information even when it operates in a more realistic non-laboratory environments where solidification or melting is not unidirectional. In this is also demonstrates a better ability to deal with real-world conditions than the sensor we proposed previously [12].

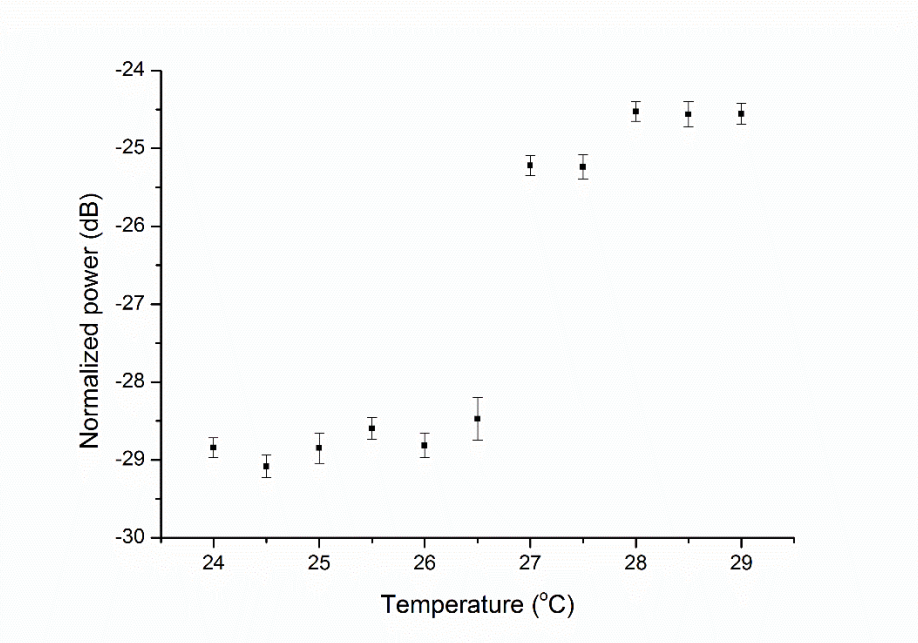


Fig.7 The result of the cooling naturally experiment.

Moreover, since the sensor is capable of detecting the phase of the sample, combined with a thermocouple, it is also capable of detecting the supercooling. As supercooling occurs, the sample maintains the liquid phase while the temperature of it is lower than the freezing point. If the output signal of the sensor is high, in the meanwhile, the temperature information got by the thermocouple shows the temperature of the sample is lower than the freezing point, the supercooling could be detected.

## Conclusion

A novel optical fiber sensor based on an SNS fiber structure for detection of the phase state of n-octadecane has been proposed and demonstrated experimentally. From the experimental results it can be seen the melting point is approximately 27.5 °C and solidification occurs at 27 °C, which is very close to the theoretical value, Since the output power level of the sensor

changes abruptly from low to high with the transition of n-octadecene from solid to liquid state (and vice versa), detection of the specific phase of the n-octadecane can be realized with a single power measurement and without the knowledge of the sample's temperature. The sensor's performance is resistant to external perturbations, such as occurrence of bubbles, impurities and mechanical disturbances. It can be easily integrated with a control unit for practical energy storage systems and is capable of detecting phase changes in many PCMs with similar to thermal-optic characteristics to n-octadecane and with the addition of a thermocouple it offers the potential to detect supercooling.

# References


1. Anderson, R. L., Adams, R. K., & Duggins, B. C. (1979). Limitations of thermocouples in temperature measurements (No. CONF-790505-14). Oak Ridge National Lab., TN (USA)
2. Akamatsu, S., Faivre, G., & Ihle, T. (1995). Symmetry-broken double fingers and seaweed patterns in thin-film directional solidification of a nonfaceted cubic crystal. *Physical Review E*, *51*(5), 4751.
3. Yin, H., & Koster, J. N. (1999). In situ observation of concentrational stratification and solid–liquid interface morphology during Ga–5% In alloy melt solidification. *Journal of crystal growth*, *205*(4), 590-606.
4. Shirtcliffe, T. G. L., Huppert, H. E., & Worster, M. G. (1991). Measurement of the solid fraction in the crystallization of a binary melt. *Journal of crystal growth*, *113*(3-4), 566-574.
5. Lazaro, A., Peñalosa, C., Solé, A., Diarce, G., Haussmann, T., Fois, M., & Cabeza, L. F. (2013). Intercomparative tests on phase change materials characterisation with differential scanning calorimeter. *Applied Energy*, *109*, 415-420.
6. Ju, Y., Ning, S., Sun, H., Mo, J., Yang, C., Feng, G., & Zhou, S. (2018). Temperature and refractive index measurement based on a coating-enhanced dual-microspheric fiber sensor. *Laser Physics*, *28*(7), 076203.
7. Tan, J., Feng, G., Zhang, S., Liang, J., Li, W., & Luo, Y. (2018). Dual spherical single-mode-multimode-single-mode optical fiber temperature sensor based on a Mach–Zehnder interferometer. *Laser Physics*, *28*(7), 075102.
8. Tian, J., Jiao, Y., Fu, Q., Ji, S., Li, Z., Quan, M., & Yao, Y. (2018). A Fabry–Perot Interferometer Strain Sensor Based on Concave-Core Photonic Crystal Fiber. *Journal of Lightwave Technology*, *36*(10), 1952-1958.
9. Liu, Y., Blokland, W., Long, C. D., Riemer, B. W., Wendel, M. W., & Winder, D. E. (2018). Strain Measurement in the Spallation Target Using High-Radiation-Tolerant Fiber Sensors. *IEEE Sensors Journal*, *18*(9), 3645-3653.
10. Millo, A., Raichlin, Y., & Katzir, A. (2005). Mid-infrared fiber-optic attenuated total reflection spectroscopy of the solid–liquid phase transition of water. *Applied spectroscopy*, *59*(4), 460-466.
11. Mani, P., Rallapalli, A., Machavaram, V. R., & Sivaramakrishna, A. (2016). Monitoring phase changes in supercooled aqueous solutions using an optical fiber Fresnel reflection sensor. *Optics express*, *24*(5), 5395-5410.

12. Han, W., Rebow, M., Liu, D., Farrell, G., Semenova, Y., & Wu, Q. (2018). Optical fiber Fresnel reflection sensor for direct detection of the solid-liquid phase change in n-octadecane. *Measurement Science and Technology*. Accepted Manuscript online 23 October 2018

13. Choi, M. K. (2016). Using Paraffin PCM to Make Optical Communication Type of Payloads Thermally Self-Sufficient for Operation in Orion Crew Module. In *14th International Energy Conversion Engineering Conference* (p. 4601).
14. Mondal, S. (2008). Phase change materials for smart textiles–An overview. *Applied thermal engineering*, *28*(11-12), 1536-1550.
15. Galione P.A., Lehmkuhl O., Rigola J., Oliva A. (2015). Fixed-grid numerical modeling of melting and solidification using variable thermo-physical properties – Application to the melting of n-Octadecane inside a spherical capsule. International Journal of Heat and Mass Transfer, Volume 86, 721-743

16. Yang, L., Xue, L., Che, D., & Qian, J. (2012). Guided-mode-leaky-mode-guided-mode fiber structure and its application to high refractive index sensing. *Optics letters*, *37*(4), 587-589.

17. Wu, Q., Semenova, Y., Wang, P., & Farrell, G. (2011). High sensitivity SMS fiber structure based refractometer–analysis and experiment. *Optics Express*, *19*(9), 7937-7944.

18. Kim, M. S., Kim, M. K., Jo, S. E., Joo, C., & Kim, Y. J. (2016). Refraction-Assisted Solar Thermoelectric Generator based on Phase-Change Lens. *Scientific reports*, *6*, 27913.

19. Jenkins, F. A., & White, H. E. (1937). *Fundamentals of optics*. Tata McGraw-Hill Education.